Am J Physiol Regul Integr Comp Physiol 312: R443–R450, 2017.
First published January 18, 2017; doi:10.1152/ajpregu.00270.2016.

RESEARCH ARTICLE | *Respiration*

Regional diaphragm volume displacement is heterogeneous in dogs

Brooke Greybeck,[1] Raymond Lu,[1] Arvind Ramanujam,[1] Mary Adeyeye,[1] Matthew Wettergreen,[2] Shari Wynd,[3] and Aladin M. Boriek[1]

[1]*Baylor College of Medicine, Houston, Texas;* [2]*Rice University, Houston, Texas; and* [3]*Texas Chiropractic College, Houston, Texas*

Submitted 24 June 2016; accepted in fina form 11 January 2017

Greybeck B, Lu R, Ramanujam A, Adeyeye M, Wettergreen M, Wynd S, Boriek AM. Regional diaphragm volume displacement is heterogeneous in dogs. *Am J Physiol Regul Integr Comp Physiol* 312: R443–R450, 2017. First published January 18, 2017; doi: 10.1152/ajpregu.00270.2016.—Muscle shortening and volume displacement (VD) are critical determinants of the pressure-generating capacity of the diaphragm. The present study was designed to test the hypothesis that diaphragm VD is heterogeneous and that distribution of VD is dependent on regional muscle shortening, posture, and the level of muscle activation. Radioopaque markers were sutured along muscle bundles of the peritoneal surface of the crural, dorsal costal, midcostal, and ventral costal regions of the left hemidiaphragm in four dogs. The markers were followed by biplanar video fluoroscop during quiet spontaneous breathing, passive inflatio to total lung capacity (TLC), and inspiratory efforts against an occluded airway at three lung volumes spanning the vital capacity [functional residual capacity, functional residual capacity + ½ inspiratory capacity, and TLC in both the prone and supine postures]. Our data show the ventral costal diaphragm had the largest VD and contributed nearly two times to the total diaphragm VD compared with the dorsal costal portion. In addition, the ventral costal diaphragm contributed nearly half of the total VD in the prone position, whereas it only contributed a quarter of the total VD in the supine postition. During efforts against an occluded airway and during passive inflatio to TLC in the supine position, the crural diaphragm displaced volume equivalent to that of the midcostal portion. Regional muscle shortening closely matched regional VD. We conclude that the primary force generator of the diaphragm is primarily dominated by the contribution of the ventral costal region to its VD.

chest wall mechanics; modeling diaphragm kinematics; respiratory muscle

MUSCLE SHORTENING, volume displacement (VD), the level of muscle activation, and posture are important determinants of the pressure-generating capacity of the diaphragm. Other investigators have studied the contribution of diaphragm muscle shortening to diaphragm VD across different ventilation maneuvers. Sprung et al. (26) measured regional muscle shortening of the diaphragm; however, the investigators did not measure diaphragm displacement and only reported data at spontaneous breathing and mechanical ventilation. In addition, Wakai et al. (28) used sonomicrometry to measure muscle shortening during quiet breathing and during more forceful breathing. In earlier studies, we evaluated the regional mechanical advantage in the diaphragm during active as well as passive volume changes (9, 29). We found a ventral to dorsal distribution of mechanical advantage that is consistent with the distribution of specifi blood flo in the costal muscle of the dog diaphragm (19). We previously determined VD of the midcostal (MC) region of the diaphragm and demonstrated that diaphragm VD is essentially proportional to muscle shortening at low lung volumes (17). At high lung volumes, diaphragm mechanical advantage decreases rapidly, and we speculated that this was due to reduced abdominal compliance or reduced volume expansion (29). While these are all critical for understanding diaphragm mechanics and kinematics, little is known on how muscle shortening affects the distribution of regional diaphragm VD. In addition, there is essentially nothing known on the contributions of regional VD to the total volume displaced by the diaphragm. It is also not known how posture and the mode of ventilation modulate regional VD of the diaphragm and, more importantly, how that affects the VD of its entire hemidiaphragm. It is important to determine the mechanical factors that interact to alter VD. Understanding the heterogeneity of VD of the diaphragm in healthy subjects may elucidate mechanisms that could explain potential changes in the heterogeneity of diaphragm VD in lung disease. Hyperinflatio of the lung in patients with chronic obstructive pulmonary disease causes the diaphragm to remodel, thus altering the physiological range of VD (25). Remodeling also changes the structural configuratio of the diaphragm, leading to heterogeneous distribution muscle lengths (27) and potentially heterogeneous VD of the diaphragm.

In this study, we tested the hypothesis that diaphragm VD is heterogeneous and that distribution of VD is dependent on regional muscle shortening, posture, and the level of muscle activation in anesthetized dogs. To test this hypothesis, we examined the contribution of different muscle regions [ventral costal (VC), MC, dorsal costal (DC), and crural (Cr)] to the total volume displaced by the left hemidiaphragm during several ventilation maneuvers in prone and supine postures. In an effort to determine the effect of lung volume on regional muscle shortening of the diaphragm, we computed regional muscle shortening and computed regional VD of the diaphragm using computational modeling techniques. Such computations were conducted during spontaneous breathing, passive inflatio to total lung capacity (TLC), and forceful inspiratory efforts during an occluded airway at functional residual capacity (FRC), FRC + ½ inspiratory capacity (½ IC), and TLC in lightly anesthetized dogs. Our data uncovered, for the firs time, a potential mechanism modulating the regional distribution of diaphragmatic VD through nonuniformity of muscle shortening of the diaphragm.

Address for reprint requests and other correspondence: A. M. Boriek, Baylor College of Medicine, One Baylor Plaza, Dept. of Medicine, Pulmonary Section, Suite 535E, Houston, TX 77030 (e-mail: boriek@bcm.edu).

METHODS

Imaging. Four female bred-for-research beagle dogs of body mass 10.1 ± 0.3 kg and inspiratory capacity 0.7 ± 0.1 liters were used for this study. Dogs were maintained according to the National Institutes of Health *Guide for the Care and Use of Laboratory Animals*, and all procedures were approved in advance by the Institutional Animal Care and Use Committee of Baylor College of Medicine. Dogs were deeply anesthetized with pentobarbital sodium (60–80 mg/kg) and surgically prepared using the same methods of our previous study (8). The abdomen was opened by midline laparotomy, and silicone-coated lead spheres were sutured onto the peritoneal surface of the left hemidiaphragm of the dogs. Three or four of those spherical markers were placed at ~1-cm intervals along six costal muscle fiber equally spaced around the circumference of the costal diaphragm. Two of these muscle bundles separated the costal diaphragm into VC, MC, and DC regions. Three to four markers were also placed along two muscle bundles of the Cr diaphragm. Animals were allowed to recover for 3–4 wk after surgery, as per Easton et al. (15). In the study by Easton and colleagues (15), minimal diaphragm tissue fibrou encapsulation was found after 3 wk of implantation, and segmental muscle shortening had stabilized after 3 wk. After recovery, animals were then anesthetized using an intravenous injection of pentobarbital sodium (Nembutal DEA Schedule II; 30 mg/kg body wt) and intubated with a cuffed endotracheal tube during the execution of all breathing maneuvers. The level of anesthesia was light based on the dosage.

Induction of respiratory loads. After the induction of anesthetic, dogs were placed in the prone or supine position in a radiolucent body plethysmograph situated in the test fiel of an orthogonal biplane fluoroscopi system. Animals were mechanically ventilated using a supersyringe until the lungs inflate to TLC, which was define as the volume at an airway pressure of 30 cmH_2O. The three-dimensional locations of the markers were obtained from a biplane video-fluoro scopic system with a high spatial (±0.5 mm) and temporal (30 Hz) resolution. Biplanar fluoroscopi images were taken at TLC. After steady, quiet breathing was resumed, images were taken at the end of expiration and end of inspiration during spontaneous breathing. The airway was then occluded at three different volumes (FRC, FRC + ½IC, and TLC), and images were taken after the dogs' fourth-sixth forceful inspiratory effort against the occluded airway. Once completed, the dog was placed in the opposite posture and the procedure was repeated.

Diaphragm modeling. The biplane fluoroscopi images taken during the respiratory maneuvers were used to determine the three-dimensional coordinates of the markers. These coordinates were imported into a nonuniform rational B-spline (NURBS) modeling software, Rhinoceros 3.0, to construct a three-dimensional model of the diaphragm to determine its surface and VD relative to FRC during the different passive and active ventilatory maneuvers.

Computation of diaphragm muscle shortening. The lengths of the three adjacent muscle fiber in the MC region of the diaphragm were computed at the reference and active states of each maneuver using the three-dimensional coordinates obtained from the biplane images. Linear distances between adjacent markers were calculated and then summed to represent the muscle fibe length. Fractional muscle shortening was computed as the ratio of the change in muscle fibe length between the reference and active states to the muscle fibe length at FRC.

Computations of diaphragm VD. To compute VD between two fitte surfaces at two different lung volumes, the modeling software is designed to compute the resulting intersection curve to an accuracy of 1/100 mm. When the surfaces intersected and actually displaced two distinct volumes VDs were decomposed into two primary components: *1*) the abdominal component is in the caudal direction and displaces the abdominal wall outward, and *2*) the ribcage component presents a lateral displacement of the diaphragm insertion on the chest wall causing an inspiratory action of the diaphragm on the ribcage. The ribcage component was termed pleural because it exerts pressure laterally on the pleural cavity. The total VD by the diaphragm was computed as the sum of these two components. The net volume displaced was computed as abdominal VD minus pleural VD. To compensate for differences in marker placement and regional diaphragm size distribution, the regions were normalized by the ratio of total diaphragm surface area at FRC to the regional surface area of the diaphragm at FRC.

Statistics. Statistical analysis was done with one-factor ANOVA tests for differences between ventilation states, lung volumes, posture, and mode of ventilation, and these variables were examined by Tukey's multiple-comparison tests. One-factor tests were used to determine the overall significanc of posture and mode of ventilation on VD. Multiple-comparison Tukey tests were performed to determine significan differences between individual groups.

RESULTS

Regional diaphragm surfaces. Surfaces were generated from radiopaque markers using NURBS (Fig. 1) to create the hemidiaphragm model and illustrate its four regions (VC, MC, DC, and Cr). The surfaces generated for each ventilation state were individually superimposed onto the FRC surface to compute volume displaced during the respiratory maneuver (Fig. 2). We have termed these components as abdominal and pleural volumes (Fig. 3). Some pairs of surfaces had no intersection, and the displaced volume was entirely abdominal.

Total VD. The data in Fig. 4 show the percent total VD of local regions of the diaphragm under various modes of ventilation (spontaneous breathing, occluded at FRC, occluded at FRC + ½IC, occluded at TLC, and passive inflatio to TLC) and in two postures [prone (*A*) and supine (*B*)]. The regional diaphragm VD relative to the total diaphragm VD did not change significantl between respiratory maneuvers in either the prone or supine postures. However, VD given by

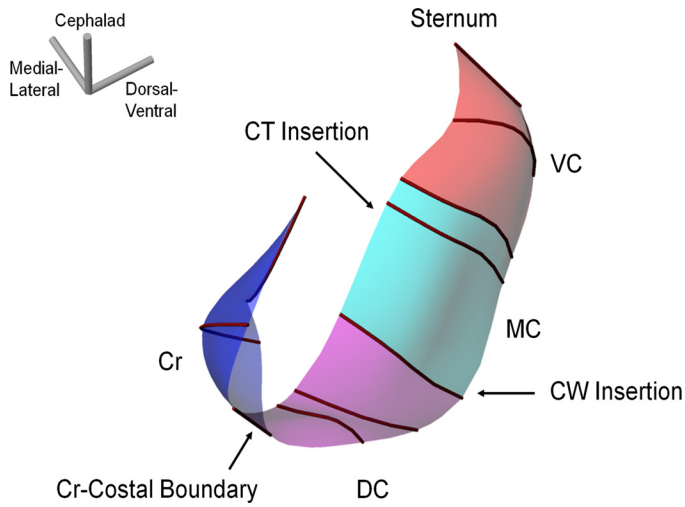

Fig. 1. Surface of the left hemidiaphragm at the end of expiration (EE) during quiet spontaneous breathing in a representative prone dog. The position of muscle fiber in each of the four regions [ventral costal (VC), midcostal (MC), dorsal costal (DC), and crural (Cr)] is shown. Nine muscle fiber (brown), excluding the Cr-costal boundary, were used to create surfaces to study volume displacement (VD) in the costal and Cr diaphragm. The central tendon (CT) insertion and chest wall (CW) insertion are also indicated on the diagram.

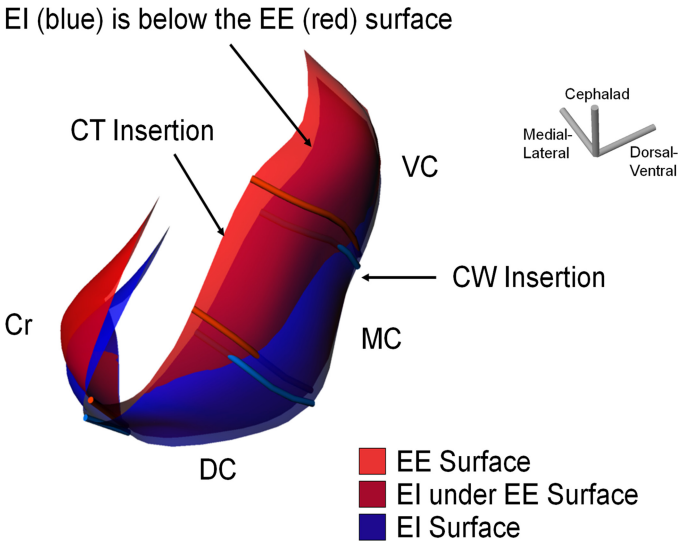

Fig. 2. Two surfaces of the diaphragm at the EE (red) and end of inspiration (EI; blue) during spontaneous quiet breathing in the same prone dog shown in Fig. 1. The surfaces were divided into the four regions of the diaphragm (VC, MC, DC, and Cr) by the muscle fiber shown. The diaphragm at the EI descends along the CT insertion site as it contracts, which is shown as being underneath the surface at the EE. This is shown in the dark red color.

each region of the diaphragm varied significantl with each other within a ventilation mode in each of the postures ($P < 0.001$).

Net VD. Net volume displaced is calculated through subtraction of the pleural volume from the abdominal volume. The data in Fig. 5 show the net volume displaced in different modes of ventilation and postures. In the prone position, we observed a significan decrease in net volume displaced by the DC portion of the diaphragm with increasing lung volumes. This suggests that in the prone position, and at higher lung volume, the dorsal diaphragm contributes most to the pleural volume displaced. In contrast, in the supine position, there were no

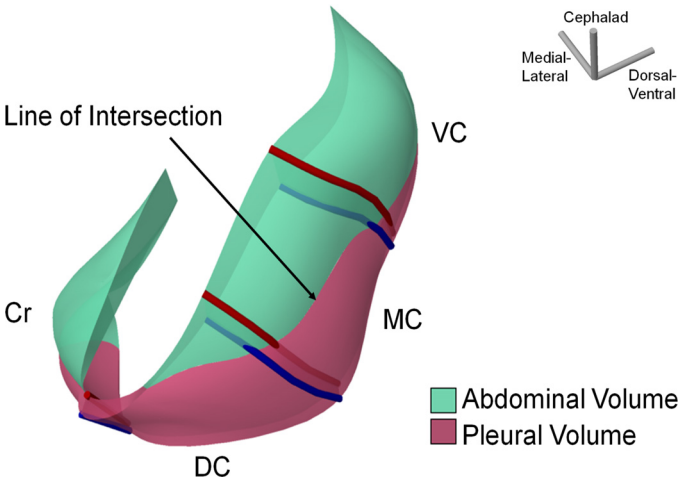

Fig. 3. Abdominal (green) and pleural (pink) volumes displaced by the diaphragm during spontaneous breathing in the same prone dog as shown in Figs. 1 and 2. The surfaces of the diaphragm at the EE (red) and EI (blue) cross along a line of intersection, thereby displacing two distinct volumes: the abdominal and pleural volumes. Note that the dorsal region of the costal diaphragm displaced the most pleural VD compared with the other regions of the diaphragm.

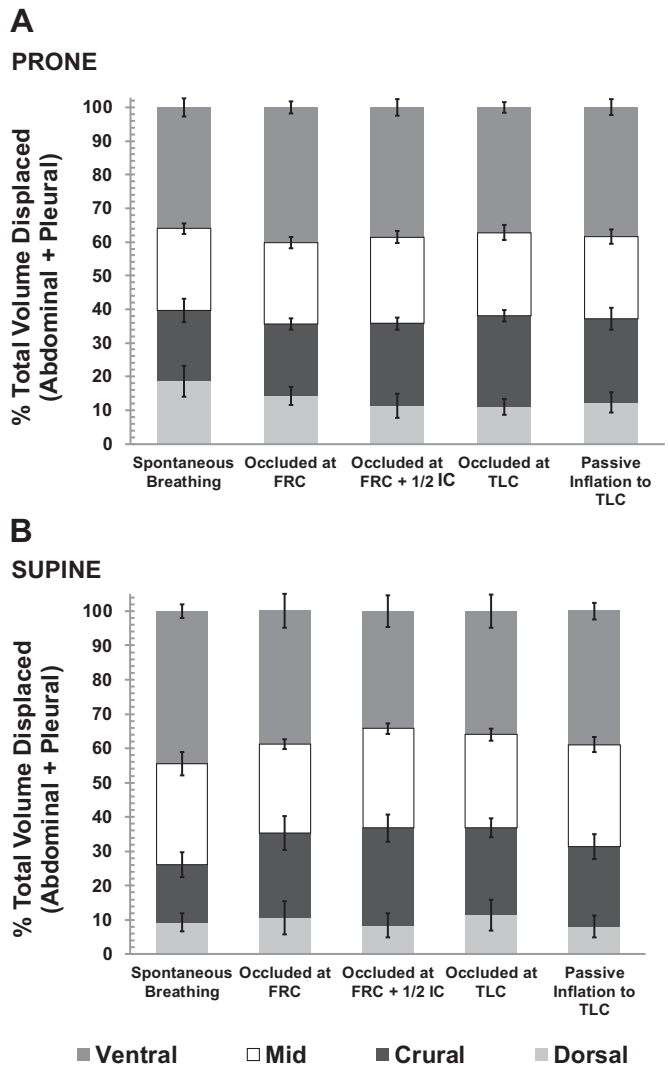

Fig. 4. Percent total volume displaced (VD) (abdominal VD + pleural VD) by the four regions of the diaphragm (VC, MC, DC, and Cr) as a function of posture (prone and supine). Total VD was determined for the each of the modes of ventilation [spontaneous quiet breathing, occluded (Occ) at functional residual capacity (FRC), occluded at functional residual capacity plus half inspiratory capacity (FRC + ½IC), occluded at total lung capacity (TLC), and passive inflatio to total lung capacity (passive TLC)]. While regional changes in total VD stayed consistent throughout changes in posture and mode of ventilation, there were apparent regional variations within each posture and ventilation state ($P < 0.001$).

significan differences in net volume displaced between respiratory maneuvers in all regions of the diaphragm. There was, however, a significan variation in volume displaced by each region of the diaphragm ($P < 0.001$).

Regional muscle shortening. Muscle fibe shortening was plotted against the location of the muscle fibe region in Fig. 6. For both postures, we determined nonuniform changes in muscle shortening with diaphragm regions under different respiratory maneuvers. The data show that muscle shortening increased during forceful efforts, against the closed airway at higher lung volume (e.g., FRC + ½IC and TLC). Furthermore, regional muscle shortening appeared to be highest at the VC-MC region in both supine and prone postures.

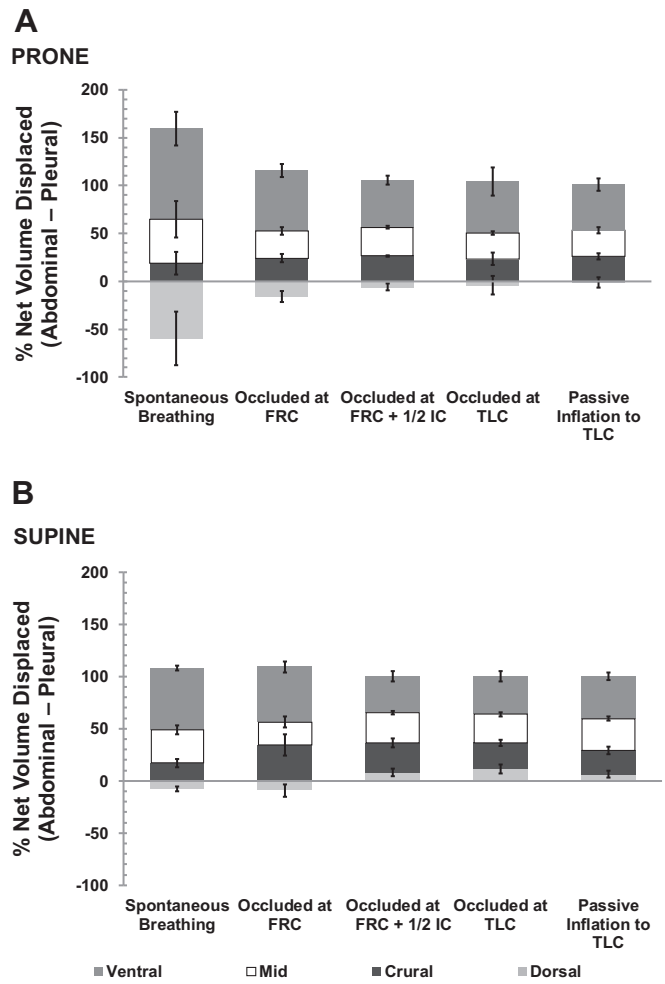

Fig. 5. Percent net volume displaced (VD) (abdominal VD – pleural VD) by the four regions of the diaphragm (VC, MC, DC, and Cr) as a function of posture [prone (*A*) and supine (*B*)] and mode of ventilation (spontaneous quiet breathing, occluded at FRC, occluded at FRC + ½IC, occluded at TLC, and passive inflatio to TLC). Error bars on both graphs represent SEs. There was a large contribution of pleural VD compared with abdominal VD in the DC portion of the diaphragm, as indicated by the negative net VD in both the prone and supine postures. During spontaneous breathing, there was significantl more contribution of the pleural VD in the prone posture compared with the supine posture ($P < 0.001$). There was a significan variation in volume displaced by each region of the diaphragm in both postures ($P < 0.001$). As lung volume increased against the occluded airway, dogs under the prone position exhibited a decrease in pleural VD in the DC region of the diaphragm. No significan changes in net volume displaced were observed as a function of mode of ventilation in the supine posture.

DISCUSSION

Our study uncovered a potential mechanism modulating the regional distribution of diaphragmatic VD through nonuniformity of muscle shortening of the diaphragm. We determined the local diaphragm regional contribution to its total VD and how diaphragm muscle shortening, mode of ventilation, and posture modulate VD. To enable lung expansion during inspiration, the diaphragm displaces volume that may be closely related to the curvature and shortening of its muscle fibers The muscle bundles that form the diaphragm are curved between their insertion points at the central tendon and chest wall, giving the diaphragm its distinctive regional curvatures and consequently its complex shape (2, 5). Each muscle fibe of the diaphragm exerts a force in the direction of its curvature, in contrast to most skeletal muscles, which exert a force along the same axis of its muscle fiber (3). We have previously shown that diaphragm muscle fiber in dogs resemble circular arcs and that when these muscle fiber shorten during contraction, they rotate around their insertion at the chest wall (8). This unique feature of diaphragm muscle kinematics allows the muscle fibe curvature to remain nearly constant, specificall in the costal region during quiet spontaneous breathing and forceful inspiratory efforts. Our previous study, which was limited to the MC diaphragm, showed that muscle fibe curvature modulated the relationship between muscle shortening and VD (17). In particular, we uncovered a nonlinear relationship between diaphragm muscle shortening and its VD, and that was due in part to a loss of diaphragm curvature at extreme muscle shortening (17). These finding complemented our data on the relationship between diaphragm muscle length and diaphragm muscle curvature, which showed that curvature was nearly constant during spontaneous breathing but decreased sharply during maximal stimulation of the diaphragm (4). We speculated that if lung compliance was increased and the chest wall and ring of diaphragm insertion were enlarged, as in the case of chronic obstructive pulmonary disease, that a signifi cant decrease in diaphragm curvature could contribute to the loss of diaphragm function (4). Although both of our earlier studies (4, 17) were limited to the MC diaphragm, they provided an important link between the level of muscle activation, diaphragm curvature, and VD. In an earlier study, we used the relationship between muscle shortening and lung volume to calculate the mechanical advantage of the diaphragm (29). In that study, we argued that with greater passive shortening, there is an increased inspiratory effect per unit σ (stress); however, with increased muscle shortening, greater displacement along the length-tension curve promotes a more pronounced change in diaphragm shape (29). Previously, we established that if tension is uniform, variations in diaphragm thickness would result in nonuniform diaphragm stress (7). In addition, Margulies et al. (22) suggested that even if the stress were uniform, variations in diaphragm thickness would affect the local curvature and thus the shape of the diaphragm. In addition, Hubmayr et al. (18) demonstrated that the shape of the diaphragm influence its efficienc to modulate transdiaphragmatic pressure. Other investigators have examined the effect of surrounding muscles and structures on the function of the diaphragm (12, 20). Leduc et al. (20) noted that to the firs approximation, the change in diaphragm length is proportional to the relative displacement of the dome and the muscle insertions into the ribs. In addition, we have recently used three-dimensional software to model the interaction between the ribs and MC diaphragm and concluded that the kinematics of the lower ribcage and its mechanical interaction with the diaphragm are more complex than previously known (12). Understanding how the diaphragm interacts with the chest wall is important in understanding the mechanics of the respiratory system. It is also important to uncover how such interaction would affect regional VD of the diaphragm. While there have been some attempts to model the diaphragm as a whole and its VD in relation to other respiratory structures (21, 23, 24), the question of how regional muscle shortening contributes to the entire volume displaced by the diaphragm remains largely

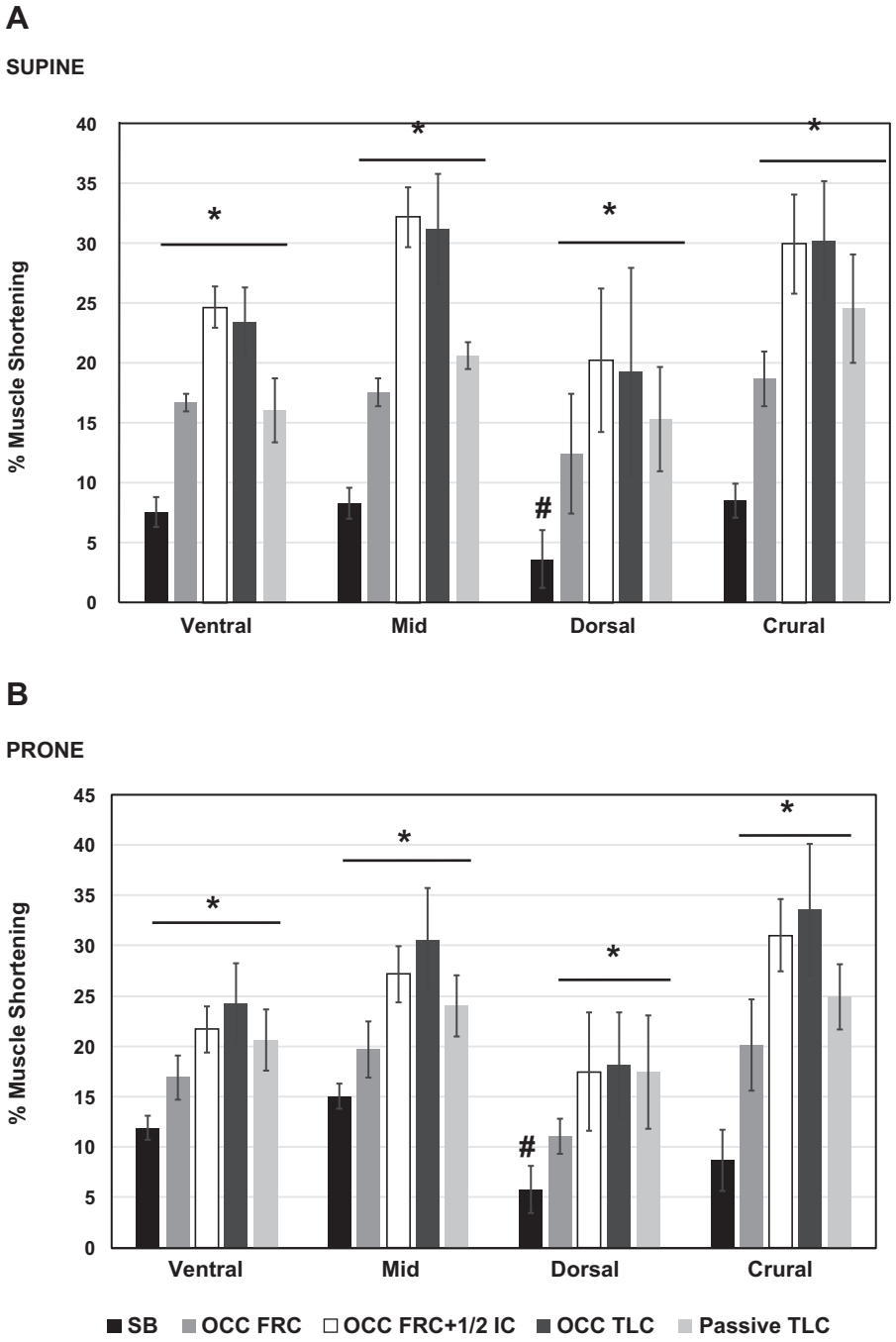

Fig. 6. Percent muscle shortening within each of the four regions (VC, MC, DC, and Cr) at two different postures [supine (*A*) and prone (*B*)]. Average percent muscle shortening was computed for all breathing maneuvers: spontaneous quiet breathing, occluded at FRC, occluded at FRC + ½IC, occluded at TLC, and passive inflatio to TLC. SEs are represented by the bars in each graph. ANOVA showed a signifi cant decrease between the percent muscle shortening during spontaneous breathing compared with all other ventilatory maneuvers in all regions of the costal and Cr diaphgram for both postures (*$P <$ 0.01). There were no significan differences in percent muscle shortening between the regions for all occluded efforts; however, there was a significan reduction of the percent muscle shortening in the dorsal region during spontaneous breathing compared with the percent muscle shortening in the other regions of the diaphragm during spontaneous breathing (#$P = 0.04$).

unknown. Therefore, we used three-dimensional modeling software to reconstruct the in vivo diaphragmatic surface to uncover the precise contributions of muscle shortening in various regions of the costal muscles (VC, MC, and DC) as well as the Cr muscle to the total diaphragm displacement.

Determinants of total regional diaphragm VD. The data in Fig. 4 show the percent contribution of the VC, MC, DC, and Cr regions to the total volume displaced by the diaphragm during different ventilation states (spontaneous breathing, forceful inspiratory efforts against an occluded airway at FRC, FRC + ½IC, TLC, and passive inflatio to TLC) in prone (*A*) and supine (*B*) postures. Total VD of the diaphragm was found as the sum of the abdominal and pleural components of VD. The regional diaphragm VD relative to total diaphragm VD did not change significantl between respiratory maneuvers in both supine and prone postures. This uniformity in total regional diaphragm VD regardless of inspiratory load and posture could be a result of a relatively constant shape of the diaphragm during inspiration. This is consistent with our finding (7, 8) that showed that diaphragm shape was similar regardless of the mode of ventilation or body position. Amancharla et al. (1) explained this phenomenon by modeling the kinematics of the active MC diaphragm and measuring displacements of the chest wall upon inspiration. They discovered that lateral displacement of the chest wall is an important mechanism for limiting the changes in the shape of the active MC diaphragm.

Other mechanisms that are at least partly responsible for constancy of diaphragm shape were explored by a finite-elemen model of the diaphragm (6). Our model suggested that changes of diaphragm shape are restricted because the central tendon is essentially inextensible and stiffness in the direction transverse to the muscle fiber is greater than stiffness along the fibe (6). Our evaluation of the regional mechanical advantage in the diaphragm during active as well as passive volume changes uncovered lower mechanical advantage of the dorsal region that is consistent with a potentially lower muscle activation of the dorsal region compared with other regions of the diaphragm (29). Our earlier data showed that muscle thickness of the dorsal region of the diaphragm is about two-thirds of the thickness in the mid- and ventral regions (10, 14), and this is consistent with smaller blood flo to the dorsal region (11).

In the present study, we demonstrated a decreased VD of the DC portion of the diaphragm in both the supine and prone positions in all modes of ventilation used in this study. Figure 4 shows that there were no significan differences in diaphragm VD between respiratory maneuvers in both postures. ANOVA showed significan variation in the percent contribution to total VD that occurred between regions within each maneuver in prone and supine postures ($P < 0.001$). Our results showed that regardless of posture, the VC diaphragm displaced the most volume during inspiration. In the prone position, the VC region contributed at least two times to total VD compared with the dorsal region. In contrast, the VC region contributed four times of the total VD of the dorsal region in the supine position. In the prone posture, the mode of ventilation did not affect the contribution of the MC portion of the diaphragm to total VD compared with the Cr region. Regardless of the mode of ventilation, both MC and Cr regions contributed similarly to total VD. In contrast, for spontaneously breathing dogs lying in the supine posture, the MC region of the diaphragm displaced a volume two times as much as the Cr region and three times that compared with the DC portion. Interestingly, during passive inflatio to TLC in the prone position, the surface of the Cr portion of the diaphragm increased and displaced volume similar to that of the MC portion. The disparity between the prone and supine postures is clearly shown by the drop in volume displaced by the DC portion of the diaphragm in the supine compared with prone posture. In contrast, there were no significan changes in total volume displaced by each region of the diaphragm in both supine and prone postures during forceful efforts against an occluded airway at increasing lung volumes.

Determinants of regional net diaphragm VD. We have shown that the contribution to total diaphragm VD by different regions of the diaphragm across various ventilation states remains fairly constant. However, our data in Fig. 5 demonstrate that the net VD is nonuniform across different levels of muscle contraction as well as passive inflatio to TLC, particularly in the prone posture. Interestingly, our data show a significan decrease in the pleural component of VD within the dorsal region of the diaphragm at passive inflatio to TLC as well as increased level of muscle activation during occluded inspiratory efforts against an occluded airway. Thus, although the total diaphragm VD in the dorsal region is relatively unchanged, the contribution of VD in the prone posture appears to be more shifted toward the abdomen relative to the pleural cavity with increasing lung volumes as well as higher level of muscle activation. This can be explained by the fact that more forceful inspiratory efforts against a closed airway at high lung volumes results in a narrowed diaphragmatic zone of apposition and reduced abdominal compliance. This directly reduces the ability of the abdominal pressure to exert an inspiratory force on the ribcage across the zone of apposition. As a result, there is a reduction in the lateral displacement of the diaphragm toward the ribcage, resulting in a reduced pleural VD.

For the supine posture, regional net volume displaced by the dorsal region of the diaphragm in spontaneously breathing dogs contributes significantl lower VD relative to the prone posture. The volume displaced by the various regions of the costal and Cr muscle in the supine posture showed no specifi pattern with changes in mode of ventilation. In the supine position, there appeared to be a small shift from lateral to abdominal displacement at higher lung volumes during a closed airway at FRC + ½IC as well as passive inflatio to TLC. This is consistent with the finding by Amancharla et al. (1), which demonstrated the ability of their diaphragm model to predict diaphragm displacement based on the hypothesis of nearly constant curvature of the diaphragm muscle fiber throughout the physiological range of ventilation in both prone and supine postures. They found that compared with the prone posture, the lateral displacement of the chest wall during inspiration was less than necessary to maintain constant curvature of the diaphragm in the supine posture. Furthermore, Wilson et al. (29) estimated that during spontaneous breathing, the diaphragm contributes ~40% of inspiratory pressure in the prone posture and ~30% in the supine posture with increased mechanical advantage for the more physiological prone posture compared with the nonphysiological supine posture. Thus, for the supine posture, reduced pleural VD in the DC region of the diaphragm results in the reduction of the dorsal region contribution to the VD of the diaphragm.

Costal versus crural VD. Our results show that the contribution of the Cr diaphragm to VD is smaller than that of the costal diaphragm muscles. Easton et al. (14) measured muscle shortening of the costal and Cr diaphragm regions as well as electromyogram activity. Although the investigators in that study did not measure VD, their observation that costal and Cr diaphragm segments exhibited differential function during chemical stimulation is consistent with our finding showing differential VD of the costal and Cr diaphragm muscles. Our data show that during spontaneous breathing, the Cr muscle displaced ~20% of the entire costal diaphragm in the prone position, whereas it contributed nearly 16% in the supine position. During passive inflatio to TLC, the Cr muscle contributed nearly 22% and 20% compared with that of the entire costal diaphragm in the prone and supine positions, respectively. These data are consistent with our earlier work showing that mechanical advantage decreased from ventral to dorsal and that the lowest mechanical advantage is in the Cr portion of the diaphragm. This also agrees well with blood flo patterns in the diaphragm (19).

Regional muscle fiber shortening. Our results show that muscle fibe shortening varies across different regions of the costal and Cr diaphragms. Particularly, percent shortening increases from the VC to MC region, where it plateaus and decreases from the MC to DC portion of the diaphragm. This resembles the percent blood flo to various portions of the

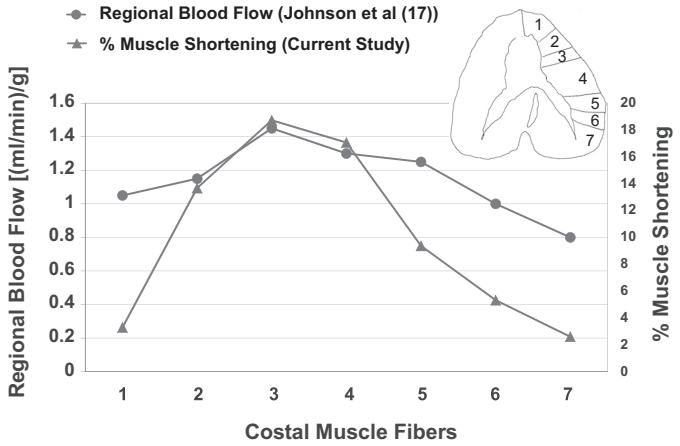

Fig. 7. Percent muscle shortening of the different regions of the costal diaphragm (refer to *inset* schematic for region identification compared with the regional blood flo per gram of muscle. Blood flo was normalized as a ratio of the regional blood flo to that measured in *costal region 7* during rest, as determined by Johnson et al. (19). Percent muscle shortening in the costal diaphragm coincided with the normalized regional blood flow with increasing muscle shortening and blood flo occurring from ventral to MC regions and then decreasing muscle shortening and blood flo from MC to dorsal regions.

diaphragm as shown by Johnson et al. (Fig. 7) (19). Diaphragm shortening corresponds to regional thickness of the diaphragm, where thickness of the dorsal muscle layer of the costal diaphragm is one-third less than the thickness displayed in the mid- and ventral regions, as reported by our earlier work (7). It is important to recognize that our data were generated using anesthetized dogs. One of the earliest studies to uncover the effect of induction of anesthesia on muscle lengths in dogs was conducted by Fitting et al. (16). The investigators in that study found clear differences between the costal and Cr diaphragms during anesthesia; the Cr segment increased its FRC lengths by nearly 7.6% after 30 min of anesthesia induction, whereas the costal muscle did not change. From these findings our shortening data of the Cr muscle but not the costal muscle could be different from awake dogs. It is also important to recognize that physiological measurements of awake dogs would have been confounded by incomplete regional recovery of the diaphgram. However, a return to anesthesia would have resolved that potential confounding influenc during the performance of breathing maneuvers (15).

Other factors affecting the heterogeneity of diaphragm VD. One of the factors that can influenc the heterogeneity of the diaphragm VD is regional differences in neural activation. Although maximal neural activation of the diaphragm was not included in this study, different levels of muscle activation from low submaximal activation during quiet breathing to higher levels of submaximal activation during occluded airway efforts were investigated. Our data in Fig. 4 did not show significan differences in regional total VD regardless of level of muscle activation. The total VD was nearly constant among different regions of the diaphragm for both supine and prone postures. Our data in Fig. 5 demonstrated that the net VD in the dorsal region was sensitive to the level of muscle activation in the physiological prone posture; however, in the supine position, the net VD did not appear to be associated with any changes regardless of the level of muscle activation. Altered gravitational loading between supine and prone positions could mediate an altered muscle activation, and thus the observed regional differences in net VD cannot be explained by muscle activation alone.

Another factor that could potentially influenc the heterogeneity of VD are the diaphragm tissue mechanics. The muscle length-tension relationship should be consistent with the transdiaphragmatic pressure-volume relationship. Thus, any alteration in the regional muscle length-tension relationship of the diaphgram may lead to altered pressure-volume relationships. Our data show that regional muscle shortening closely matched regional VD.

The mechanical interaction between the lower ribcage, diaphragm, and abdominal wall is another determinant of diaphragm VD. Our data in Fig. 5 show net VD calculated through subtraction of the pleural volume from the abdominal volume at different breathing maneuvers. During normal spontaneous breathing in the supine position, there appears to be minimal differences between pleural and abdominal VD, whereas in the prone position, pleural VD is much greater than abdominal VD.

Perspectives and Significance

Our study has shown that regional differences in diaphragm VD are modulated by changes in posture, mode of ventilation, and muscle shortening. In particular, we showed nonuniform contributions of different regions of the diaphragm to total VD. The ventral region of the costal diaphragm muscle has the greatest contribution to total VD compared with other regions of the diaphragm. In addition, the contribution of total VD by each region remains nearly constant irrespective of posture or mode of ventilation. Since net VD is a good measure of the ratio of lateral to caudal displacement, a large negative net VD is correlated with more lateral movement of the chest wall expanding the ribcage, whereas a positive net VD is associated with greater caudal displacement of the diaphragm pushing the abdomen wall outward. In the physiological prone posture, the DC portion of the diaphragm exhibited a large contribution to net VD. Yet, our data show a significantl lower contribution to net VD by the dorsal diaphragm in the nonphysiological supine position. Additionally, the same lateral diaphragm VD in the DC portion of the prone posture exhibited a decrease in VD that corresponds to increasing lung volume. Our results show that regional muscle shortening of the diaphragm was nonuniform and closely matched the total and net VD distribution of those regions of the diaphragm. Muscle shortening was higher in the VC and MC regions of the diaphragm, and percent muscle shortening dropped significantl in the DC region of the diaphragm. This correlates well with our previous study on the regional effects of the diaphragm on its mechanical advantage. In particular, our data on muscle shortening are consistent with the regional blood flo patterns of the diaphragm shown in Fig. 7 (19). This suggests that although the DC portion is important for exerting inspiratory effect on the chest wall, most of the force-generating power and also VD of the diaphragm needed to generate pressure is developed by the VC portion of the diaphragm. Our study provides new insights on the importance of regional muscle shortening to efficien pump function. Our data demonstrate that diaphragm VD is heterogeneous and that its distribution is consistent with the distribution of mechanical advantage of the diaphragm high-

lighted in our earlier work (29). The heterogeneous distribution of VD and muscle shortening are consistent with blood flo heterogeneity during exercise in both dogs (19) and ponies (21). Future studies that are designed to investigate how regional muscle shortening contributes to VD during exercise would be timely. Such studies could pave the way to uncover mechanisms that are responsible for the limited exercise capacity and compromised inspiratory function in patients with lung disease such as chronic obstructive pulmonary disease. Our finding may also be important for understanding diaphragm function and blood flo in patients with a single lung transplant or lung resection (13). Taken together, our study supports the observation that regional mechanics of the diaphragm with respect to VD and muscle shortening provides new insights on important determinants of how the complex structure of the diaphragm contributes to its function.

GRANTS

This work was funded by National Institutes of Health Grants RO1-HL-072839 and R25-HL-108853 as well as the National Science Foundation.

DISCLOSURES

No conflict of interest, financia or otherwise, are declared by the author(s).

AUTHOR CONTRIBUTIONS

B.G. and A.M.B. drafted manuscript; R.L., A.R., M.A., M.W., S.W., and A.M.B. analyzed data; R.L. and A.M.B. interpreted results of experiments; R.L., S.W., and A.M.B. prepared figures M.A., S.W., and A.M.B. edited and revised manuscript; S.W. and A.M.B. approved fina version of manuscript; A.M.B. performed experiments.

REFERENCES

1. **Amancharla MR, Rodarte JR, Boriek AM.** Modeling the kinematics of the canine midcostal diaphragm. *Am J Physiol Regul Integr Comp Physiol* 280: R588–R597, 2001.
2. **Angelillo M, Boriek AM, Rodarte JR, Wilson TA.** Shape of the canine diaphragm. *J Appl Physiol* 89: 15–20, 2000.
3. **Angelillo M, Boriek AM, Rodarte JR, Wilson TA.** Theory of diaphragm structure and shape. *J Appl Physiol* 83: 1486–1491, 1997.
4. **Boriek AM, Black B, Hubmayr R, Wilson TA.** Length and curvature of the dog diaphragm. *J Appl Physiol* 101: 794–798, 2006. doi:10.1152/japplphysiol.00865.2004.
5. **Boriek AM, Liu S, Rodarte JR.** Costal diaphragm curvature in the dog. *J Appl Physiol* 75: 527–533, 1993.
6. **Boriek AM, Rodarte JR.** Effects of transverse fibe stiffness and central tendon on displacement and shape of a simple diaphragm model. *J Appl Physiol* 82: 1626–1636, 1997.
7. **Boriek AM, Rodarte JR.** Inferences on passive diaphragm mechanics from gross anatomy. *J Appl Physiol* 77: 2065–2070, 1994.
8. **Boriek AM, Rodarte JR, Wilson TA.** Kinematics and mechanics of midcostal diaphragm of dog. *J Appl Physiol* 83: 1068–1075, 1997.
9. **Boriek AM, Rodarte JR, Wilson TA.** Ratio of active to passive muscle shortening in the canine diaphragm. *J Appl Physiol* 87: 561–566, 1999.
10. **Boriek AM, Wilson TA, Rodarte JR.** Displacements and strains in the costal diaphragm of the dog. *J Appl Physiol* 76: 223–229, 1994.
11. **Brancatisano A, Amis TC, Tully A, Kelly WT, Engel LA.** Regional distribution of blood flo within the diaphragm. *J Appl Physiol* 71: 583–589, 1991.
12. **Chu I, Fernandez C, Rodowicz KA, Lopez MA, Lu R, Hubmayr RD, Boriek AM.** Diaphragm muscle shortening modulates kinematics of lower rib cage in dogs. *Am J Physiol Regul Integr Comp Physiol* 299: R1456–R1462, 2010. doi:10.1152/ajpregu.00016.2010.
13. **De Troyer A, Leduc D.** Effects of single-lung inflatio on inspiratory muscle function in dogs. *J Physiol* 576: 269–277, 2006. doi:10.1113/jphysiol.2006.112797.
14. **Easton PA, Abe T, Smith J, Fitting JW, Guerraty A, Grassino AE.** Activity of costal and crural diaphragm during progressive hypoxia or hypercapnia. *J Appl Physiol* 78: 1985–1992, 1995.
15. **Easton PA, Fitting JW, Arnoux R, Guerraty A, Grassino AE.** Recovery of diaphragm function after laparotomy and chronic sonomicrometer implantation. *J Appl Physiol* 66: 613–621, 1989.
16. **Fitting JW, Easton PA, Arnoux R, Guerraty A, Grassino A.** Effect of anesthesia on canine diaphragm length. *Anesthesiology* 66: 531–536, 1987. doi:10.1097/00000542-198704000-00014.
17. **Greybeck BJ, Wettergreen M, Hubmayr RD, Boriek AM.** Diaphragm curvature modulates the relationship between muscle shortening and volume displacement. *Am J Physiol Regul Integr Comp Physiol* 301: R76–R82, 2011. doi:10.1152/ajpregu.00673.2010.
18. **Hubmayr RD, Sprung J, Nelson S.** Determinants of transdiaphragmatic pressure in dogs. *J Appl Physiol* 69: 2050–2056, 1990.
19. **Johnson RL Jr, Hsia CC, Takeda S, Wait JL, Glenny RW.** Efficien design of the diaphragm: distribution of blood flo relative to mechanical advantage. *J Appl Physiol* 93: 925–930, 2002. doi:10.1152/japplphysiol.00230.2002.
20. **Leduc D, Cappello M, Gevenois PA, De Troyer A.** Mechanics of the canine diaphragm in ascites: a CT study. *J Appl Physiol* 104: 423–428, 2008. doi:10.1152/japplphysiol.00884.2007.
21. **Macklem PT.** A mathematical and graphical analysis of inspiratory muscle action. *Respir Physiol* 38: 153–171, 1979. doi:10.1016/0034-5687(79)90034-3.
22. **Margulies SS.** Regional variation in canine diaphragm thickness. *J Appl Physiol* 70: 2663–2668, 1991.
23. **Mead J, Loring SH.** Analysis of volume displacement and length changes of the diaphragm during breathing. *J Appl Physiol Respir Environ Exerc Physiol* 53: 750–755, 1982.
24. **Petroll WM, Knight H, Rochester DF.** A model approach to assess diaphragmatic volume displacement. *J Appl Physiol (1985)* 69: 2175–2182, 1990.
25. **Ruel M, Deslauriers J, Maltais F.** The diaphragm in emphysema. *Chest Surg Clin N Am* 8: 381–399, 1998.
26. **Sprung J, Deschamps C, Hubmayr RD, Walters BJ, Rodarte JR.** In vivo regional diaphragm function in dogs. *J Appl Physiol* 67: 655–662, 1989.
27. **Supinski GS, Kelsen SG.** Effect of elastase-induced emphysema on the force-generating ability of the diaphragm. *J Clin Invest* 70: 978–988, 1982. doi:10.1172/JCI110709.
28. **Wakai Y, Leevers AM, Road JD.** Regional diaphragm shortening measured by sonomicrometry. *J Appl Physiol* 77: 2791–2796, 1994.
29. **Wilson TA, Boriek AM, Rodarte JR.** Mechanical advantage of the canine diaphragm. *J Appl Physiol* 85: 2284–2290, 1998.